Thermal Dynamics and a Comparison of the Thermal Stability of Various Non-Wood Pulps

Youmao Zhang,[a] Kefu Chen,[a] Jinquan Wan,[a] Haolian Zhuo,[b] Jichen Li,[b] Rendang Yang,[a] Wenguang Yang,[a] Fei Yang,[a,c] and Bin Wang [a,c] *

Specialty paper products made using natural pulps is an attractive field for the paper industry and for researchers. Studying the thermal dynamics of plant pulps is an important step toward improving the thermal stability of papers. This study has the aim of gaining detailed insight into the thermal properties of softwood, hardwood, flax, hemp, mulberry, bamboo, bagasse, and esparto pulps. Chemical composition and thermogravimetric analyses of these non-wood pulps were performed to find the correlations between the chemical, structural, and thermal properties of these pulps. In addition, the Malek model for kinetics of the thermo-decomposition process of pulps is proposed. The kinetics of the most probable mechanism function for $G(\alpha) = 1-(1-\alpha)^{1/2}$ of the thermo-decomposition process of plant fibers from 200 to 400 °C is deduced using the Malek model. This study also provides a method to help select the most promising pulps for specialty materials.

Keywords: Pulps; Thermal dynamics; Malek model

Contact information: a: School of Light Industry and Food Sciences, South China University of Technology, Guangzhou, 510640, China; b: Technology Center, China Tobacco Guangdong Industrial Co., Ltd., Guangzhou 510385, China; c: Key Lab of Paper Science and Technology of Ministry of Education, Qilu University of Technology, Jinan, Shandong Province 250353, China;
** Corresponding author: febwang@scut.edu.cn*

INTRODUCTION

With the expansion of paper application fields, the requirement for specific types of paper with specific functions has arisen. Such specific types of paper include capacitor paper, insulation paper, and archival paper (Gui *et al.* 2013; Huang *et al.* 2013; Zhu *et al.* 2013). These papers need to have resistance to both high heat and aging. Temperature is one of the main factors affecting the thermal stability performance of papers. With an increase in temperature, the volatile compounds of a fiber are broken up into small molecular hydrocarbons and expelled. In the course of such thermal decomposition the glycosidic linkage of cellulose is broken, the polymerization degree is reduced, and the aging resistance is weakened. Therefore, the key way to improve aging resistance is by raising the thermal stability of papers.

Pulp, the major component of paper, plays an important role in papermaking technology. The performance of pulp directly correlates with the aging and heat-resistance properties of a given paper. The pulp is derived from a variety of plant fibers whose characteristic properties, such as their species, location, origin (leaf, bast, bole, and stem) and age, should be considered. In general, non-wood plant pulps that are generated in large quantities, such as flax, hemp, bamboo, bagasse, and esparto fibers, are also used in the papermaking industry (Marques *et al.* 2010; Alila *et al.* 2013). However, there is little

information about the chemical, thermal, and morphological properties of non-wood pulp for papermaking.

Cellulose, lignin, and hemicellulose are the three main components in all natural fibers (Yang *et al.* 2006). The differences in their chemical composition and structure cause the differences in their chemical behavior as well as in the pyrolysis process. In fact, there has been a lot of research on nature fibers for their thermal properties (Chattopadhyay *et al.* 2011; Elkhaoulani *et al.* 2013). Moriana *et al.* (2014) summarized the correlations between thermal properties and chemical composition among different nature fibers. Through the thermogravimetric methodology, they assessed the thermal property of fibers in relation to their chemical composition and proposed the potential application for thermal conversion or material reinforcements. Marques *et al.* (2010) evaluated the chemical composition of different non-woody plant fibers for using in pulp and paper manufacturing. They mainly analyzed the influence of chemical composition on the pulping and bleaching performances. However, the correlation of chemical composition and thermal properties of pulps were not mentioned.

Information about their functional properties, which is related to their complex composition, is essential when attempting to use the pulp as a raw material to produce paper. Therefore, each chemical component should be analyzed to predict the relationship between their chemical structure and the thermal degradation process.

The thermal stability and thermal degradation kinetics are other important aspects to consider when using natural pulps as materials to make heat-resistant paper. To date, the study of heat-resistant paper has mostly aimed at original, rather than processed, pulp. Hence, it is important to analyze the chemical composition and physical properties and carry out the thermogravimetric analysis of pulp. Furthermore, there are only a few studies that have focused on the heat resistance of pulp, and little information is available on the pyrolysis mechanism. In this work the chemical structure and thermal properties of softwood, hardwood, flax, hemp, mulberry, bamboo, bagasse, and esparto pulps were evaluated, aiming to screen better resources for development of heat-resistant pulps for applications in the papermaking process.

EXPERIMENTAL

Materials

Softwood, hardwood, flax, hemp, mulberry, bamboo, bagasse, and esparto pulps were the selected commercial pulps (bleached chemical pulp), provided by Hua Feng paper Co., Ltd. (Shanghai, China). The physical and mechanical properties of the pulps are summarized in Table 1.

Chemical Composition Analysis

The chemical composition of each pulp was determined according to the procedures reported in previous works (Kataki and Konwer 2001; Yasuda *et al.* 2001; Schwanninger *et al.* 2004; Zhang *et al.* 2012; Frollini *et al.* 2013).

The extraction of each pulp using a benzene-ethanol solution (2:1 in volume) as the solvent was carried out for 6 h in a Soxhlet apparatus. The amount of the extractives was determined according to the difference in weight loss. The cellulose content was determined by the nitrate method. Extracted pulp (1 g) was refluxed and extracted at 100 °C for 1 h using 25 mL of mixed ethyl alcohol and nitric acid (4:1 in volume) as the solvent.

Table 1. Physical and Mechanical Properties of Each Pulp

	Fiber length[1] (mm)			Fiber width[1] (μm)	Fiber curl[1] (%)	CrI	
	L(n)	*L*(l)	*L*(w)			H_{1429}/H_{893}[2]	$(I_{002}-I_{AM})/I_{002}$[3]
Softwood	0.34	0.89	2.02	14.33	16.8	0.77	0.60
Hardwood	0.31	0.85	1.83	14.77	17.6	0.81	0.64
Flax	0.41	1.21	1.81	14.29	24.8	0.67	0.55
Hemp	0.36	0.74	1.11	12.25	10.0	0.83	0.70
Mulberry	0.38	0.73	1.14	16.3	9.3	0.72	0.58
Esparto	0.69	2.02	3.08	18.95	17.9	0.70	0.57
Bamboo	0.85	1.81	2.39	22.98	15.7	0.79	0.63
Bagasse	0.62	0.87	1.02	15.21	13.7	0.66	0.54

[1] Measured with a Kajaani FS 300 (Mesto, Finland)
[2] Calculated from infrared spectrum by FTIR (Nicolet, NEXUS 470, USA)
[3] Calculated from X-ray diffraction pattern by diffractometer (Bruker D8 Advance, Germany)

The insoluble lignin content of pulp was measured using the Klason method. Samples were first hydrolyzed with 72 w/w % sulfuric acid at 20 °C for 2 h. The acid was then diluted with water to a concentration of 3 w/w% sulfuric acid, and the mixture was boiled for 4 h. The resulting material was cooled to the room temperature and filtered. The dry weight of the solids was measured as acid-insoluble lignin content. The acid-soluble lignin was measured by UV spectrophotometry (Agilent 8453, USA) at 320 nm.

The holocellulose content (cellulose + hemicellulose) was determined as follows: 0.6 g of $NaClO_2$, 0.5 mL of glacial acetic acid, and 65 mL of deionized water were mixed and added to 2 g of extracted pulp at 75 °C for 1 h. Then, 0.6 g of $NaClO_2$ and 0.5 mL of glacial acetic acid were added every hour until the pulp turned white. The resulting material was cooled and filtered. The hemicellulose content was determined by subtracting the percentage of cellulose from the percentage of holocellulose.

The total ash content of the pulp was measured after combustion at 575 ± 25 °C. Three replications for each pulp were performed, and the results were averaged.

Fourier-Transform Infrared Spectrometry (FTIR)

FTIR was used to investigate molecular structures and to obtain information regarding the cellulose crystalline domains from the functional groups. The FTIR spectra of each pulp were acquired on a Nexus 470 spectrophotometer (Thermo Nicolet, USA). The dry samples were mixed and ground with KBr for IR measurement in the wavenumber range of 400 to 4000 cm^{-1}. The relative contents of the crystalline allomorph of each pulp were identified using the second derivatives of the FTIR spectra.

X-Ray Diffraction (XRD) Measurement

The pulps were analyzed on a D8 ADVANCE diffractometer (Bruker, Germany) equipped with a Cu Kα filtered radiation (λ = 0.154 nm) and operating at a voltage of 40 kV and a current density of 40 mA. Scans were collected from 2θ = 10° to 40° at a scan rate of 2°/s and a step width of 0.02°. The crystalline index (I_{CR}) of cellulose in each pulp was computed from the XRD patterns using the Segal empirical method (Chen *et al.* 2006),

$$I_{CR} = 1 - \frac{I_{AM}}{I_{002}} \quad (1)$$

where I_{AM} is the amorphous counter reading at the valley (near 18°) and I_{002} is the counter reading at the maximum (at 22°).

Thermal Analyses

The thermal decomposition of the pulp was evaluated by thermogravimetric analysis (TGA). TGA was performed with a NETZSCH TG 209 Jupiter Thermal Analysis System (TA Instruments, USA) thermogravimetric analyzer under an air atmosphere (50 mL/min). The samples were heated from 25 to 650 °C at a heating rate of 10 °C/min.

Thermal Degradation Kinetics

The kinetic parameters: apparent activation energy (*E*), and the pre-exponential factor (*A*) were determined from Coats–Redfern method (Ebrahimi-Kahrizsangi and Abbasi 2008). According to the linear relationship of the equation, *E* and *A* were obtained from slope and *Y*-intercept, respectively. The apparent activation energy *E*, and pre-exponential factor (*A*) were applied to evaluate the thermal degradation kinetics of each pulp in the individual thermal decomposition process.

RESULTS AND DISCUSSION

Chemical Composition Analyses

The chemical composition and the behavior of wood and non-wood pulps during pyrolysis is important to their pyrolysis behavior. The results in earlier experiments showed that the decomposition of hemicellulose occurred earliest during pyrolysis, followed by the decomposition of cellulose; lignin was the most difficult to decompose (Yang *et al.* 2007). Hemicellulose is rich in branches that are easy to remove, and cellulose is made of thousands of glucose molecules linked into giant chains without any branches, while lignin has a heterogeneous structure that causes its degradation to be extremely difficult. Therefore, the thermal stability of cellulose is higher than hemicellulose and lower than lignin (Dorez *et al.* 2013).

Table 1 presents the carbohydrate composition of various pulps. The results show that these fibers had differences in their chemical compositions. These pulps contained less lignin because the lignin removal technology was implemented during the pulping process. Therefore, in this work, we focus on the roles of cellulose and hemicellulose. Hemp pulp had the highest cellulose content (80.31%) and the lowest hemicellulose content (2.11%). The preliminary conclusion is that hemp pulp has high thermal stability. In addition, previous research shows that bast fibers, such as flax and jute, with high cellulose content, can be considered potentially competitive with aramid fibers (Moriana *et al.* 2014).

Table 2. Chemical Composition of Woody and Non-wood Pulps

	Softwood	Hardwood	Flax	Hemp	Mulberry	Esparto	Bamboo	Bagasse
Cellulose (%)	67.97	72.21	75.56	80.31	72.81	64.52	70.75	64.55
Hemicellulose (%)	18.96	12.23	7.26	2.11	7.85	11.26	14.23	5.89
Lignin (%)	2.48	4.21	1.10	2.12	4.23	2.28	1.52	0.87
Extractives (%)	2.43	4.88	2.17	4.26	3.42	0.96	4.21	1.14
Ash content (%)	0.56	0.97	2.43	3.55	3.55	2.79	3.13	3.24

Fourier Transform Infrared Spectrometry

Figure 1 presents the FTIR spectra of hardwood, softwood, flax, hemp, mulberry, bamboo, bagasse, and esparto pulps to elucidate the chemical structure of each pulp. The absorption peaks in the region around 3500 cm^{-1} are an indication of the stretching of hydrogen–bonded OH groups. The vibration absorption peaks around 2900 cm^{-1} result from the C-H stretching vibration. FTIR results did present a large difference in terms of the chemical structures of these pulps.

There was a difference in the regions of the C-H stretching vibrations because of the differing chemical constituents of the given pulps. Using this information, the crystallinity index (CrI) from the infrared spectroscopy based on the relative intensity was evaluated.

The vibration absorption peaks at 1429 and 893 cm^{-1} are characteristic peaks of the crystalline and amorphous regions in the cellulose (Kljun *et al.* 2011). The height ratio (H1429/H893) was used to determine the CrI of cellulose material (Ragab *et al.* 2014). Table 1 summarizes the values of CrI for all pulps. The CrI values followed the same trend for the pulps. Bagasse, esparto, and flax showed lower cellulose percentages, exhibiting lower crystallinity indexes than the others. Hemp, with a high cellulose content, showed the highest CrI.

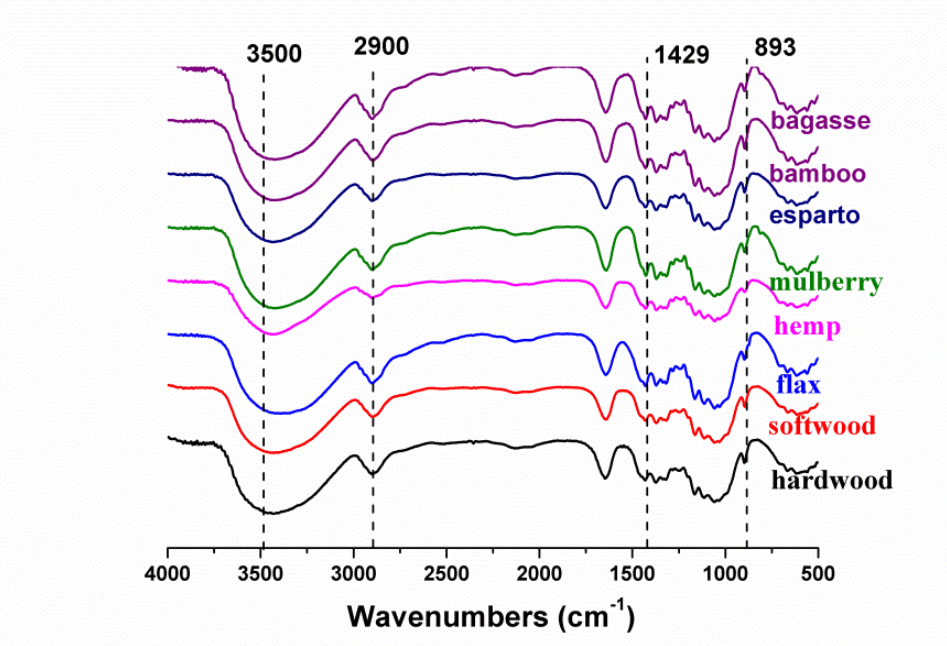

Fig. 1. FTIR spectra of the pulps

X-Ray Scattering

The X-ray diffraction profiles of the pulps are shown in Fig. 2. The XRD pattern for all pulps clearly showed strong diffraction maxima (2θ) at approximately16.5° and 22.6°. The occurrence of these signals indicates that pulps exhibit a typical cellulose-I X-ray pattern (Ouajai and Shanks 2005). The crystallinity index and degree of crystallinity of each pulp are shown in Table 1. The same trend of CrI values was also observed in FTIR results (Fig. 1) for the pulps. Hemp and hardwood pulps, with high cellulose contents, showed higher crystalline indexes than other pulps.

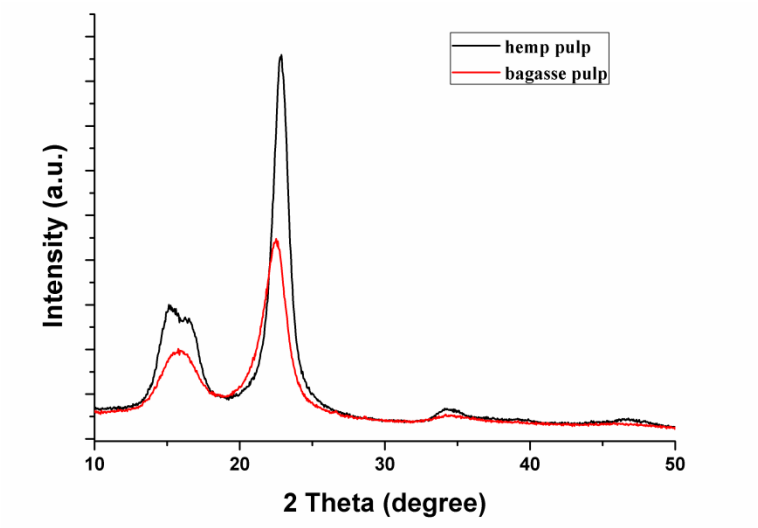

Fig. 2. X-ray diffraction of representative pulps

Thermal Analyses

In this section, thermal pyrolysis experiments for each pulp were carried out to investigate their pyrolysis behavior in a TG apparatus. The weight loss curves of the pulps are given in Fig. 3. As can be seen, the first mass-loss regions for the pulps were in the section with temperatures from 25 to 200 °C. This was attributed to the release of water absorbed with a weight loss ratio between 3.05 to 8.48 wt.% in the pulps.

The second mass-loss region was between 200 and 400 °C, and the weight loss was mostly due to the depolymerization of hemicellulose and cellulose. The most weight loss occurred in this region. The main peak of the DTG curve was attained near 350 °C and was attributed to the degradation of cellulose and hemicellulose. From the DTG curve it is apparent that the decomposition temperature was primarily related to the cellulose content (Moriana *et al.* 2014). Esparto and bagasse pulps exhibited low cellulose contents and low decomposition temperatures (264.2 and 279.2 °C, respectively). Hemp and flax pulps exhibited higher thermal stability and higher decomposition temperatures (288.5 and 288.5 °C, respectively) due to the higher content of crystalline cellulose which is the most thermal stable component of fibers (Barneto *et al.* 2011). In general, higher cellulose content in the natural fibers exhibit higher thermal stability. This is very attractive to be applied as heat-resisting paper due to their resistance to degradation during heating or service life.

The last stage of mass loss was at temperatures higher than 400 °C. Little residue (approximately 10 wt.% of the original weight) remained at 600°C. The TGA results show that the water was removed at temperature of about 150 °C for all the pulps. The weight loss for all the pulps was negligible from 150 °C to 200 °C, while the weight of pulps was gradually reduced after 200 °C. In order to eliminate the difference caused by different water contents for different pulps, normalization processing was carried out for thermal analyses. The TGA curves were normalized to 100 wt.% at initial weight of 200 °C, and the results are shown in Fig. 3.

Table 3 shows the characteristic parameters of the TGA-DTG curves of pyrolysis of pulp. The temperature (T_{max}) of maximum weight loss rates in descending order were hemp pulp > flax pulp > softwood pulp > bamboo pulp > mulberry pulp > hardwood pulp > esparto pulp > bagasse pulp. The T_{max} of hemp pulp was the highest (368.1 °C), and bagasse pulp had the lowest temperature of maximum loss-weight (345.4 °C). The T_{max} of flax pulp

was 367.0 °C, which was similar to the 361.4 °C of hardwood pulp. The hardwood, mulberry, bamboo, and esparto pulps had similar T_{max} readings, around 355 °C. In the process of pyrolysis, a high T_{max} suggests high energy consumption and better thermal stability. The data in Table 3 indicate that hemp, flax, and hardwood pulps have greater thermal stability than other pulps.

The hemp pulp had the highest T_{max} (368.3 °C), which was similar to the flax pulp (367.0 °C), and bagasse pulp had the lowest temperature of maximum loss-weight (345.4 °C). The hardwood, softwood, mulberry, bamboo, and esparto pulps had similar T_{max}, from 354.2°C to 361.4 °C. But the temperatures of T_W, $T_{0.05}$, $T_{0.1}$, and $T_{0.5}$ for different pulps showed no obvious pattern.

In summary, from the above results, it can be approximately concluded that the hemp, flax, hardwood, and mulberry pulps had greater thermal stability than softwood, esparto, bamboo, and bagasse pulps.

Table 3. Thermogravimetric Parameters of Various Pulps

Pulp	T_W (°C)	$T_{0.05}$ (°C)	$T_{0.1}$ (°C)	$T_{0.5}$ (°C)	T_{max} (°C)
Softwood	272.1	289.1	306.6	352.2	355.2
Hardwood	284.9	301.9	318.9	358.0	361.4
Flax	288.5	304.6	321.6	363.2	367.0
Hemp	288.5	305.5	322.5	363.6	368.3
Mulberry	287.2	305.0	322.7	354.2	355.2
Esparto	264.2	282.9	303.9	353.9	354.2
Bamboo	281.1	296.3	311.3	351.8	354.5
Bagasse	279.2	295.1	307.5	344.1	345.4

$T_{0.05}$, $T_{0.1}$, and $T_{0.5}$: temperature at the rate of weight loss of 5%, 10% and 50%

Thermal Degradation Kinetics

In this section, a pyrolysis mechanism is proposed to account for the thermal degradation kinetics of the pulps using kinetics equations.

The general form for solid decomposition is usually defined as:

$$\frac{d\alpha}{dt} = k\, f(\alpha) \quad (1)$$

$$G(\alpha) = kt \quad (2)$$

where α is conversion, t is time, and $f(\alpha)$ and $G(\alpha)$ are the mathematical functions that are present in the mechanism function. The conversion rate (a) can be calculated according to the thermogravimetric curve of pulps.

$$\mathrm{a} = \frac{m_0 - m}{m_0 - m_\infty} \quad (3)$$

In the above equation, m_0, m, and m_∞ represent the initial (at 200 °C), instantaneous and final (at 400 °C) weights of pulps, respectively. The reaction rate constant k can be obtained based on the Arrhenius equation as:

$$k = A\, exp(-\frac{E}{RT}) \quad (4)$$

Combining Eqs. 1 and 4 gives:

$$\frac{d\alpha}{dt} = A\, f(\alpha) exp(-\frac{E}{RT}) \quad (5)$$

For constant heating rate non-isothermal conditions ($\beta=dT/dt$), Eq. 5 is frequently rearranged as,

$$\beta \frac{d\alpha}{dt} = A\, f(\alpha) exp(-\frac{E}{RT}) \quad (6)$$

where β is the heating rate. Integration of Eq. 6 leads to,

$$G(\alpha) = \int_0^{\alpha} \frac{d\alpha}{f(\alpha)} = \frac{A}{\beta}\int_0^{T} exp(-\frac{E}{RT})\ dT = \frac{ART^2}{E\beta}\exp(-\frac{E}{RT}) \quad (7)$$

where $G(\alpha)$ is the integral form of the reaction model, A is the pre-exponential factor, E is the activation energy, and R is the molar gas constant.

To evaluate the thermal degradation kinetics of the pulps, the Malek method was selected to deduce the kinetic model.

Combining Eqs. 6 and 7 yields:

$$G(\alpha) = \frac{RT^2}{E\beta}\ \frac{\mathrm{d}\alpha}{\mathrm{d}t}\ \frac{1}{f(\alpha)} \quad (8)$$

When α = 0.5,

$$G(0.5) = \frac{RT_{0.5}^2}{E\beta}\ (\frac{\mathrm{d}\alpha}{\mathrm{d}t})_{0.5}\ \frac{1}{f(0.5)} \quad (9)$$

where $T_{0.5}$ and $(\mathrm{d}\alpha/\mathrm{d}t)_{0.5}$ are the temperature and reaction rate, respectively, when α = 0.5.

The defined function $y(\alpha)$ = Eq. 8/Eq. 9 gives:

$$y(\alpha) = (\frac{\mathrm{T}}{T_{0.5}})^2\ \frac{(\frac{\mathrm{d}\alpha}{\mathrm{d}t})}{(\frac{\mathrm{d}\alpha}{\mathrm{d}t})_{0.5}} = \frac{f(\alpha)\cdot G(\alpha)}{f(0.5)\cdot G(0.5)} \quad (10)$$

$$y(\alpha) = \frac{f(\alpha)\cdot G(\alpha)}{f(0.5)\cdot G(0.5)} \quad (11)$$

which corresponds to each reaction mechanism shown in Table 4, and,

$$y(\alpha) = (\frac{\mathrm{T}}{T_{0.5}})^2\ \frac{(\frac{\mathrm{d}\alpha}{\mathrm{d}t})}{(\frac{\mathrm{d}\alpha}{\mathrm{d}t})_{0.5}} \quad (12)$$

which can be obtained from TGA data. The $y(\alpha)$ -α curves of Eqs. 11 and 12 represent standard curves and experimental (EC) curves, respectively.

Representative curves of softwood pulp, which degraded between between 200 and 400 °C, are shown in Fig.4. The y(a) curves of E_n, F_n, R_4, R_3, R_2, $R_{1/2}$, $R_{1/3}$, $R_{1/4}$, D_1, D_2, D_3, D_4, P_n, and A_n were plotted using Eq. 11 according to different reaction mechanisms (Table 4). The y(a) curve of EC was plotted using Eq. 12 according to the TGA results of softwood pulp with heating rate of 10 °C/min.

It is clear that the experimental (EC) curve of representative hardwood pulps nearly overlapped the standard curves $R_{1/2}$ (as seen in Fig. 4). It was concluded that the most probable mechanism function of pulp was the phase interfacial reaction. Additionally, the kinetic mechanism function was $G(\alpha) = 1 - (1-\alpha)^{1/2}$ and the reaction order was second-order.

Calculation of Activation Energy

The Coats–Redfern method is considered to be a helpful solution to determine the activation energy E and pre-exponential factor A for pulps (Ebrahimi-Kahrizsangi and Abbasi 2008). The dynamic equation is:

$$\ln[\frac{G(\alpha)}{T^2}] = \ln\left(\frac{AR}{\beta E}\right) - \frac{E}{RT} \quad (13)$$

Using the linear relationship of the equation $\ln[G(\alpha)/T^2] - 1/T$, E and A were obtained based on thermogravimetry, where the two variables are the slope and y intercept, respectively. The results are shown in Table 5.

The thermal degradation kinetic fitting equation among the eight kinds of pulp in Table 5 was in keeping with the correlation coefficient R > 0.98. The apparent activation energy of thermal decomposition of the pulps in descending order was: mulberry > softwood > hemp > bagasse > hardwood > bamboo > flax > esparto.

The apparent activation energy of mulberry pulp was 137.74 kJ/mol, which was the highest among the eight pulps. The lowest was esparto pulp, with 99.83 kJ/mol. These results are similar to the Broido-Shafizadeh model and other literature (Bradbury *et al.* 1979).

A high pulp apparent activation energy suggests a high stability. In summary, the above results demonstrated that the mulberry pulp and bamboo pulp had higher thermal stability, while the esparto pulp had the lowest thermal stability.

Table 4. Algebraic Expressions of Functions of the Most Common Reaction Mechanisms

Number	Mechanism	Symbol	*f(α)*	*G(α)*
1	One-dimensional diffusion	D_1	$1/2\alpha$	α^2
2	Second-dimensional diffusion	D_2	$-1 / \ln(1-\alpha)$	$\alpha + (1-\alpha)\ln(1-\alpha)$
3	Third-dimensional diffusion (Jander)	D_3	$3(1-\alpha)^{2/3} / \{2[1-(1-\alpha)^{1/3}]\}$	$[1-(1-\alpha)^{1/3}]^2$
4	Third - dimensional diffusion	D_4	$3/\{2[(1-\alpha)^{-1/3}-1]\}$	$1-2\alpha/3-(1-\alpha)^{2/3}$
5	Nucleation and growth (JMA)	A_n	$n(1-\alpha)[-\ln(1-\alpha)]^{1/(1-n)}$	$[-\ln(1-\alpha)]^{1/n}$
6	Phase interfacial reaction	R_n	$n(1-\alpha)^{1-1/n}$	$1-(1-\alpha)^{1/n}$
7	Chemical reaction	F_n	$(1-\alpha)^n$	$[1-(1-\alpha)^{1-n}]/(1-n)$
8	Power function	P_n	$n\,\alpha^{(n-1)/n}$	$\alpha^{1/n}$
9	Exponential function	E_n	α/n	$\ln(\alpha^n)$

The chemical composition, temperature of maximum weight loss, and apparent activation energy of thermal decomposition are all related to the thermal stability of pulp. So the higher the content of cellulose has, the higher will be the T_{max} of the pulp, which leads to a higher apparent activation energy during thermal decomposition process. However, there was some deviation in the results shown in Tables 1, 2, and 5.

Possible explanations for the deviations are as follows: (1) apart from containing cellulose, the pulp also contains hemicellulose, lignin, and other organic or inorganic substances. Therefore, the degradation and interaction of these substances influences the thermal degradation of pulp, which causes some inconsistency between the temperature of maximum weight loss and the content of cellulose; (2) during the weight loss process of pulp, the factors that affect thermal decomposition were not limited only to dynamic factors, but also other factors like heat or mass transfer. Therefore, the apparent activation energy calculated from this dynamic model was not fully consistent with the decomposition temperature.

Table 5. Pyrolysis Equations and Thermodynamic Parameters of Pulps

Sample	Fitted equation	R	*E* (kJ/mol)	*A* (s^{-1})
Softwood	y = -139603.20x + 8.50	-0.9879	116.01	1.14×10^{7}
Hardwood	y = -15565.88x + 10.76	-0.9947	129.35	1.22×10^{8}
Flax	y = -17357.32x + 13.36	-0.9905	144.24	1.83×10^{9}
Hemp	y = -18049.85x + 14.71	-0.9938	149.99	7.36×10^{9}
Mulberry	y = -16575.74x + 12.65	-0.9898	137.74	8.62×10^{8}
Esparto	y = -12013.31x + 5.36	-0.9901	99.83	4.26×10^{5}
Bamboo	y = -13828.36x + 8.08	-0.9921	114.91	7.45×10^{6}
Bagasse	y = -12258.65x + 8.05	-0.9915	101.87	6.40×10^{6}

In summary, the thermal stability of pulp was mostly determined by the apparent activation energy. Therefore, from the above results, it can be concluded that the thermal stability of the eight pulps in descending order was hemp > flax > mulberry > hardwood > softwood > bamboo > bagasse > esparto. The result is approximately consistent with the cellulose content of eight pulps.

As shown above, the composition of pulps could affect the crystalline states of cellulose. In addition, more energy needs to be consumed to destroy the crystalline region during the process of pyrolysis. Hence, extra energy consumption caused higher thermal stability.

These results were in agreement with previous research which showed that pure cellulose has better thermal stability than lignocellulosic fibers (Chang *et al.* 2014). Therefore, the chemical compositions of pulp were the main criteria in deciding the thermal stability of pulp.

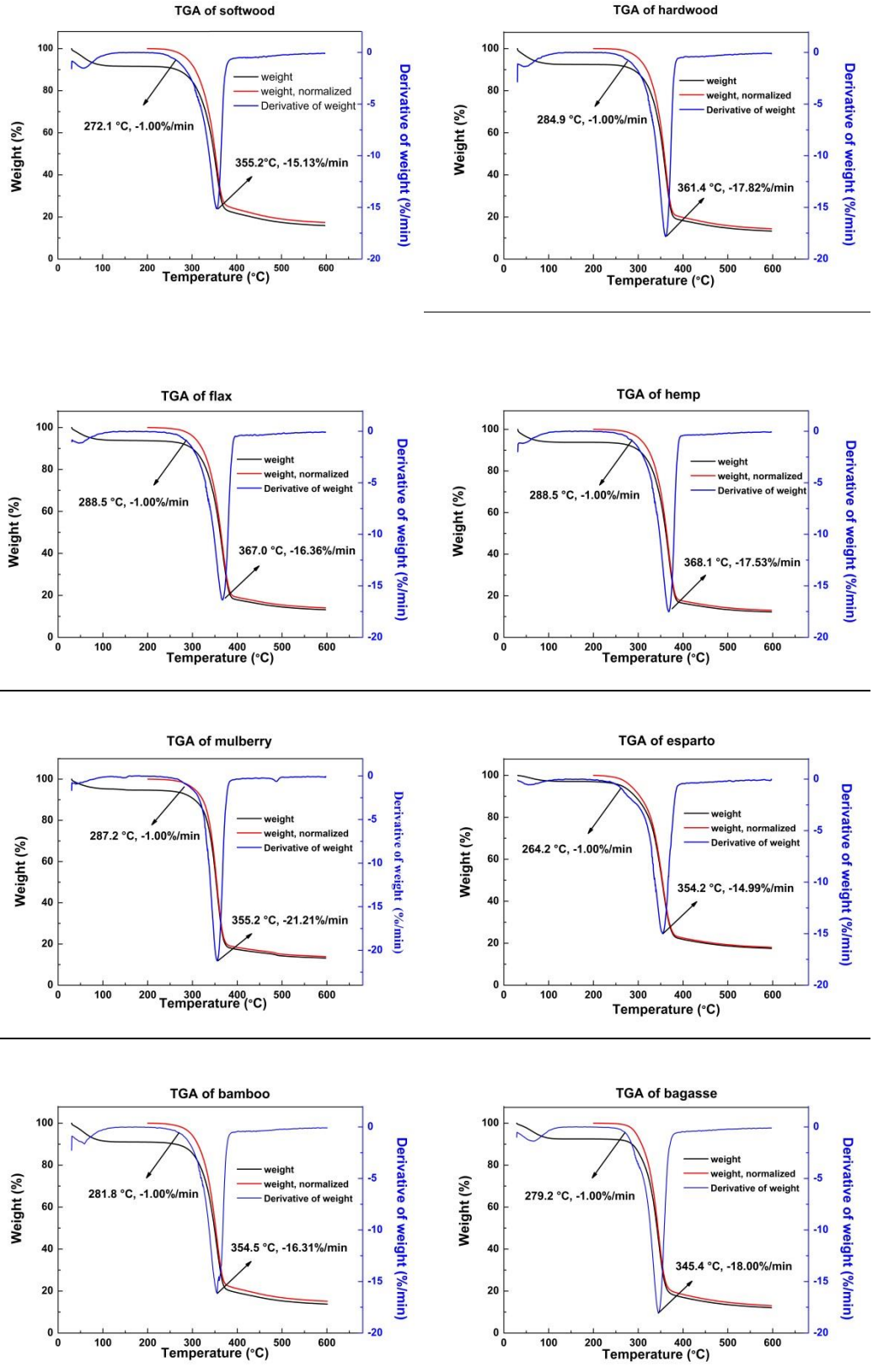

Fig. 3. Thermogravimetric and derivative curves of the pulps

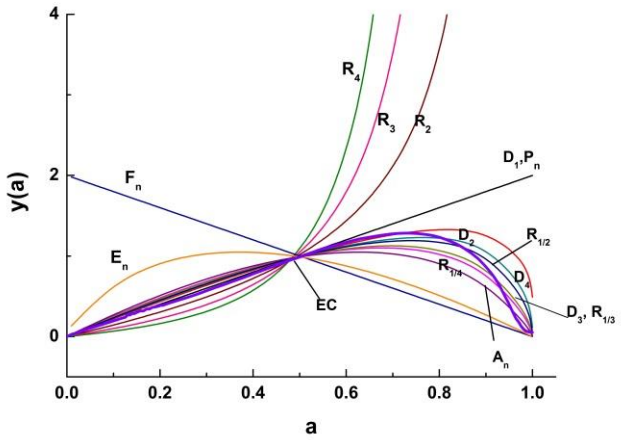

Fig. 4. Masterplots of different kinetic models calculated by the Malek method for representative hardwood.

CONCLUSIONS

1. The thermal weight loss process of pulps from 30 °C to 600 °C was found to include three stages. The range of temperature of the main thermal degradation process was 200 °C to 400 °C, and the residue weight was approximately 10 wt.% at 600 °C. The decomposition temperatures of T_W, $T_{0.05}$, $T_{0.1}$, $T_{0.5}$, and T_{max} indicated that the hemp, flax, hardwood, and mulberry pulps had greater thermal stability than softwood, esparto, bamboo and bagasse pulps.
2. Using the Malek method of the thermal degradation dynamic mechanism function to draw an inference, the thermal degradation of the pulp could be described as a phase interfacial reaction. The reaction order is second-order. The dynamic mechanism function is $G(\alpha) = 1 - (1-\alpha)^{1/2}$. Using the Coats-Redfern method to fit the thermal degradation dynamic equation, the correlation coefficients were all > 0.98.
3. The fibers with higher cellulose content (hemp and flax) showed higher structural properties and thermal stability. Combined with the results of decomposition temperature and the apparent activation energy of thermal decomposition, the stability measurements of eight pulps in descending order were hemp pulp > flax pulp > mulberry pulp > hardwood pulp > softwood pulp > bamboo pulp > esparto pulp > bagasse pulp.

ACKNOWLEDGMENTS

The authors are grateful for the support of the Natural Science Foundation of Guangdong Province (2015A030310369 & 2015A030313221) and the Foundation (No. 0308031363 & 0308031367) of Key Laboratory of Pulp and Paper Science and Technology of Ministry of Education (Qilu University of Technology).

REFERENCES CITED

Alila, S., Besbes, I., Vilar, M. R., Mutjé, P., and Boufi, S. (2013). "Non-woody plants as raw materials for production of microfibrillated cellulose (MFC): A comparative study," *Industrial Crops and Products* 41, 250-259. DOI: 10.1016/j.indcrop.2012.04.028

Barneto, A. G., Vila, C., Ariza, J., and Vidal, T. (2011). "Thermogravimetric measurement of amorphous cellulose content in flax fibre and flax pulp," *Cellulose* 18(1), 17-31. DOI: 10.1007/s10570-010-9472-0

Bradbury, A. G., Sakai, Y., and Shafizadeh, F. (1979). "A kinetic model for pyrolysis of cellulose," *Journal of Applied Polymer Science* 23(11), 3271-3280. DOI: 10.1002/app.1979.070231112

Chang, Y. C., Choi, D., Takamizawa, K., and Kikuchi, S. (2014). "Isolation of *Bacillus* sp. strains capable of decomposing alkali lignin and their application in combination with lactic acid bacteria for enhancing cellulase performance," *Bioresource Technology* 152, 429-436. DOI: 10.1016/j.biortech.2013.11.032

Chen, X., Burger, C., Fang, D., Ruan, D., Zhang, L., Hsiao, B. S., and Chu, B. (2006), "X-ray studies of regenerated cellulose fibers wet spun from cotton linter pulp in NaOH/thiourea aqueous solutions," *Polymer* 47(8), 2839-2848. DOI: 10.1016/j.polymer.2006.02.044

Dorez, G., Taguet, A., Ferry, L., and Lopez-Cuesta, J. M. (2013). "Thermal and fire behavior of natural fibers/PBS biocomposites," *Polymer Degradation and Stability* 98(1), 87-95. DOI: 10.1016/j.polymdegradstab.2012.10.026

Ebrahimi-Kahrizsangi, R., and Abbasi, M. (2008), "Evaluation of reliability of Coats-Redfern method for kinetic analysis of non-isothermal TGA," *Transactions of Nonferrous Metals Society of China* 18(1), 217-221. DOI: 10.1016/S1003-6326(08)60039-4

Elkhaoulani, A., Arrakhiz, F., Benmoussa, K., Bouhfid, R., and Qaiss, A. (2013). "Mechanical and thermal properties of polymer composite based on natural fibers: Moroccan hemp fibers/polypropylene," *Materials & Design* 49, 203-208. DOI: 10.1016/j.matdes.2013.01.063

Frollini, E., Bartolucci, N., Sisti, L., and Celli, A. (2013). "Poly (butylene succinate) reinforced with different lignocellulosic fibers," *Industrial Crops and Products* 45, 160-169. DOI: 10.1016/j.indcrop.2012.12.013

Gui, Z., Zhu, H., Gillette, E., Han, X., Rubloff, G. W., Hu, L., and Lee, S. B. (2013). "Natural cellulose fiber as substrate for supercapacitor," *ACS Nano* 7(7), 6037-6046. DOI: 10.1021/nn401818t

Huang, J., Zhu, H., Chen, Y., Preston, C., Rohrbach, K., Cumings, J., and Hu, L. (2013). "Highly transparent and flexible nanopaper transistors," *ACS Nano* 7(3), 2106-2113. DOI: 10.1021/nn304407r

Kataki, R., and Konwer, D. (2001), "Fuelwood characteristics of some indigenous woody species of north-east India," *Biomass and Bioenergy* 20(1), 17-23. DOI: 10.1016/S0961-9534(00)00060-X

Kljun, A., Benians, T. A., Goubet, F., Meulewaeter, F., Knox, J. P., and Blackburn, R. S. (2011). "Comparative analysis of crystallinity changes in cellulose I polymers using ATR-FTIR, X-ray diffraction, and carbohydrate-binding module probes," *Biomacromolecules* 12(11), 4121-4126. DOI: 10.1021/bm201176m

Marques, G., Rencoret, J., Gutiérrez Suárez, A., and d. Río Andrade, J. C. (2010). "Evaluation of the chemical composition of different non-woody plant fibers used for pulp and paper manufacturing," *The Open Agriculture Journal* 4, 93-101. DOI: 10.2174/1874331501004010093

Moriana, R., Vilaplana, F., Karlsson, S., and Ribes, A. (2014), "Correlation of chemical, structural and thermal properties of natural fibres for their sustainable exploitation," *Carbohydrate Polymers* 112, 422-431. DOI: 10.1016/j.carbpol.2014.06.009

Ouajai, S., and Shanks, R. (2005). "Composition, structure and thermal degradation of hemp cellulose after chemical treatments," *Polymer Degradation and Stability* 89(2), 327-335. DOI: 10.1016/j.polymdegradstab.2005.01.016

Ragab, T. I., Wasfy, A., Amer, H., El-Gendi, A., Abdel-Hady, M., and Liebner, F. (2014). "Synthesis of cellulose acetate membrane from the Egyptian rice straws," *Journal of Applied Sciences* 14(24), 3424-3435. DOI: 10.3923/jas.2014.3424.3435

Schwanninger, M., Rodrigues, J., Pereira, H., and Hinterstoisser, B. (2004). "Effects of short-time vibratory ball milling on the shape of FT-IR spectra of wood and cellulose," *Vibrational Spectroscopy* 36(1), 23-40. DOI: 10.1016/j.vibspec.2004.02.003

Yang, H., Yan, R., Chen, H., Zheng, C., Lee, D. H., and Liang, D. T. (2006). "In-depth investigation of biomass pyrolysis based on three major components: Hemicellulose, cellulose and lignin," *Energy & Fuels* 20(1), 388-393. DOI: 10.1021/ef0580117

Yang, H., Yan, R., Chen, H., Lee, D. H., and Zheng, C. (2007). "Characteristics of hemicellulose, cellulose and lignin pyrolysis," *Fuel* 86(12), 1781-1788. DOI: 10.1016/j.fuel.2006.12.013

Yasuda, S., Fukushima, K., and Kakehi, A. (2001). "Formation and chemical structures of acid-soluble lignin I: Sulfuric acid treatment time and acid-soluble lignin content of hardwood," *Journal of Wood Science* 47(1), 69-72. DOI: 10.1021/ef0580117

Zhang, H., Pang, H., Shi, J., Fu, T., and Liao, B. (2012). "Investigation of liquefied wood residues based on cellulose, hemicellulose, and lignin," *Journal of Applied Polymer Science* 123(2), 850-856. DOI: 10.1002/app.34521

Zhu, H., Jia, Z., Chen, Y., Weadock, N., Wan, J., Vaaland, O., Han, X., Li, T., and Hu, L. (2013). "Tin anode for sodium-ion batteries using natural wood fiber as a mechanical buffer and electrolyte reservoir," *Nano Letters* 13(7), 3093-3100. DOI: 10.1021/nl400998t

Article submitted: September 10, 2015; Peer review completed: October 16, 2015; Revised version received and accepted: December 27, 2015; Published: January 19, 2016.
DOI: 10.15376/biores.11.1.2138-2151